Arraid Journal of Science and Technology (AJST)
Higher Institute of Science and Technology-Al Shmokh

مجلة الرائد للعلوم والتقنية
المعهد العالي للعلوم والتقنية ـ الشموخ

Received: 15 October 2025 | Accepted: 25 November 2025 | Published online: 30 December 2025

A CFD Analysis of Winglet Angle Effects on the Hover Performance of a Helicopter Rotor

Hweda M. Shairf*, Ali Mohamed Belhaj, Salim A. Shawesh***
*Technical College of Civil Aviation, Esbea, Libya
** Higher Institute of Science and Technology, Zahraa, Libya
hwedasharif@gmail.com, Ali.belhag@yahoo.com, Alshaweshsalim2@gmail.com

ABSTRACT

This study numerically investigates the aerodynamic performance of a UH-60A Black Hawk rotor blade equipped with winglets under hover conditions. The primary objective is to evaluate the potential for performance improvement by analyzing various winglet angles and directions. Computational Fluid Dynamics (CFD) simulations were conducted using NUMECA, solving the Reynolds-Averaged Navier-Stokes (RANS) equations with the Spalart-Allmaras turbulence model. The results indicate that the incorporation of winglets yields a modest increase in rotor thrust of approximately 2%. However, this thrust enhancement is accompanied by an increase in torque across all tested winglet configurations, indicating a concomitant rise in power requirement.

KEYWORDS: Helicopter rotor blade, CFD, winglet, hover condition, Winglet.

1. INTRODUCTION

The application of winglets, a proven technology for fixed-wing aircraft to reduce induced drag, has been extensively studied for helicopter rotor systems. The primary motivation is to improve rotor aerodynamic efficiency, which directly translates to increased payload, extended range, better hover performance, and reduced fuel consumption. Unlike fixed wings, the helicopter rotor operates in a highly complex, unsteady aerodynamic environment with transonic flow on the advancing side and dynamic stall on the retreating side. This study was started in July 1976, when Whitcomb [1 , 2], NASA Langley Research Centre published a study that mentioned some design approaches, which briefly mentioned and explained the aerodynamic technology called as the winglet design. The study mentioned that some little but vertically arranged fins should be installed on the KC-135A aircraft wings. They were tested during the years 1979 and 1980. The winglet was capable of carrying aerodynamic loads. The vortex was caused when the winglet spread out that decreased the downwash, which resulted in further reduction in the induced drag as compared to the area increase in the profile drag. Whitcomb proved that the tiny winglets had the capacity to raise an aircraft's range by up to 7% of the cruise speeds. This process reduced the induced drag and increased the profile drag when the airspeed increased.

In 1980s, a NASA contract [3] reassessed winglets as well as other drag reducing devices, and discovered that wingtip devices including winglet, sails and feathers were

effective for improving drag as the lift efficiency increased 10-15% in case when those wingtip devices are integrated with the wing design. Mark D. [4] proposed a new winglet design and predicted their performance (SAILPLANES) as they had good agreement with the results of the flight-test; however, the designs were tested for very limited time.

Monier ElFarra conducted a study [5], in which, he pointed out that if a winglet is added to a wind turbine blade, which points towards the blade's suction side; it will generate more power. For understanding the process of reducing the drag with the help of the winglet, the difference between the induced drag and the profile drag must be understood. The profile drag takes place because of the viscosity caused by the air that moves on the airfoil surface and also because of the pressure drag. When the wind turbine blades move in that viscous air, some air sticks to the blades while the remaining continues its motion. The air requires the blade's energy to rotate with the blade, so when this energy transfers from the blade to the air, it causes the profile drag.

Moreover, some other factors also result in the profile drag such as the blade's wetted area, the attack angle and the blade's airfoil shape [6 and 7]. The induced drag also occurs because of the lift caused by the blade. When the lift exists, the blade sides should have pressure difference. These sides are distinguished based on the pressure such as the pressure side and the suction side (lower pressure side). The pressure difference causes span-wise flow from the pressure side towards the suction side, which can be felt all along the trailing edge because the flow that leaves the suction side shifts inwards. On the other hand, the flow coming from the pressure side shows an outward movement. These are two opposing flows but when they meet each other on the trailing edge, their collision results in a swirling motion, which is concentrated on the known tip vortices. The vortices are generated with the help of energy, which transfers from the blade to the air. This energy transfer is called as induced drag that can be decreased when the span-wise flow is reduced. The winglets help reducing it [1].

When a winglet is added to a helicopter blade, it produces a flow that opposes the airflow generated by the blade. Hence, it cancels or at least weakens the blade's main flow reducing the span wise flow, which, consequently, reduces the induced drag.

The [8] it was concluded that adding a winglet to a wing increases its aerodynamic efficiency in terms of CL/CD. A winglet's function is to diffuse the tip vortex effect; so, it decreases the induced drag; however, adding a winglet increases the wetted area that further increases the profile drag. It is possible to design a winglet in many geometrical shapes/variations, which might result in optimizing the aerodynamic efficiency of a wing during varying flight conditions in addition to reducing fuel consumption and pollution.

2. METHODOLOGY

This paper discusses the outcomes of the simulations of 3-D steady state Computational Fluid Dynamics (CFD) by presenting test case UH-60A Black Hawk helicopter rotor, which was used for testing in the hovering conditions.. The test case was considered for validating the commercial NUMECA CFD software. The standard 3D RANS equations in a rotating frame of reference is as follows:

$$\frac{\partial}{\partial t}\int_V Q\, dV + \oint_S (\mathbf{F}\cdot\mathbf{n})\, dS - \oint_S (\mathbf{F_v}\cdot\mathbf{n})\, dS = \int_V s_T\, dV \quad (1)$$

Where: Q is the vector of conservative variables, $\mathbf{F}$ is the invicid flux, $\mathbf{F_v}$ is the viscous flux and s_T is the source term. Those vectors are given by:

$$Q = \begin{Bmatrix} \bar{\rho} \\ \bar{\rho}\,\tilde{u}_1 \\ \bar{\rho}\,\tilde{u}_2 \\ \bar{\rho}\,\tilde{u}_3 \\ \bar{\rho}\,\tilde{e}_0 + k \end{Bmatrix} \quad (2)$$

$$\mathbf{F} = \begin{Bmatrix} \bar{\rho}\,\tilde{w}_j \\ \bar{\rho}\,\tilde{w}_1\tilde{w}_j + \bar{p}\delta_{1j} \\ \bar{\rho}\,\tilde{w}_2\tilde{w}_j + \bar{p}\delta_{2j} \\ \bar{\rho}\,\tilde{w}_3\tilde{w}_j + \bar{p}\delta_{3j} \\ \bar{\rho}\,\bar{h}_0\tilde{w}_j + k\,\tilde{w}_j \end{Bmatrix} \quad \boldsymbol{F_v} = \begin{Bmatrix} 0 \\ \tilde{\tau}_{1j} - \tau^T_{1j} \\ \tilde{\tau}_{2j} - \tau^T_{2j} \\ \tilde{\tau}_{3j} - \tau^T_{3j} \\ \tilde{u}_i\,\tilde{\tau}_{ij} - \tilde{q}_j + \Theta^T_j \end{Bmatrix} \quad (3)$$

$$s_T = \begin{Bmatrix} 0 \\ -\bar{\rho}(\boldsymbol{\omega}\times\mathbf{u}) \\ 0 \end{Bmatrix} \quad (4)$$

Where w is the relative velocity, u is the absolute velocity, ρ is the density, e_0 is total energy, p is the pressure, h_0 is total enthalpy, k is the kinetic energy of turbulent fluctuations, τ^T_{ij} is the Reynolds stress tensor, Θ^T_j consists of the turbulent heat flux tensor q^T_j and other turbulent terms evolving from density-velocity correlations and triple velocity correlations of the turbulent fluctuations, δ_{ij} is the Kronecker delta and ω is the angular velocity.

2.1. Blade Description and the Real Data

Because of the flow-field periodicity, just a single blade was considered and the periodic boundary condition was implemented on the other blades. The blade features and geometric dimensions were taken using a scale of (1: 5:73) as shown in [9].

The data was acquired for a 9:4ft 2.9 m diameter, four-blade scale (1: 5:73) of UH-60A rotor. A UH-60A rotor blade consists of two different airfoils distributed as follow: SC1095 airfoil in the root and tip regions and the SC1094R8 airfoil in the mid-span region as shown in Figure (1).

The mentioned blade possesses unique twist distribution as Figure (2) shows. The blade twist distribution has a linear shape as r/R < 0.75 while it is non-linear on the tip. The blade has a built-in twist that linearly varies in the 80% blade radius, and it has hook-like non-linear twist closer to the tip, which is part of the model. Moreover, the blade's elastic twist applies the measured defections [9]. A blade pitch distribution having a built-in, collective, and elastic twist can be plotted against the radius and compared to the experimental results as shown in Figure (2). In addition, there is also a 20^o rearward sweep beginning at r/R = 0:93. The average chord is 3.64in (0.0924m) that produces a 15:3 blade aspect ratio and 0.0825 solidity ratio.

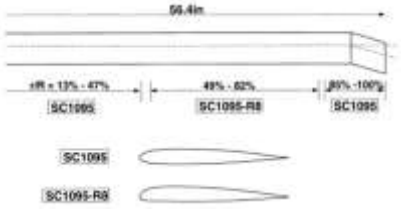

Figure 1: Blade and airfoil shape of UH-60A black hawk rotor [10].

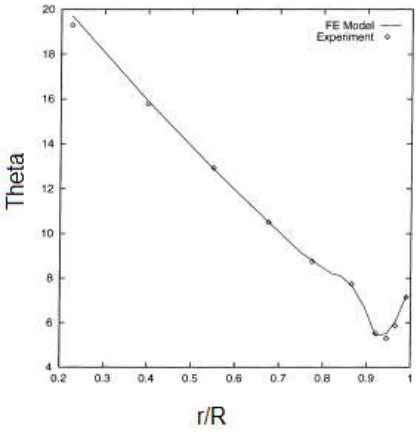

Figure 2: The twist distribution of UH-60 blade [11].

2.2. Geometrical shapes for a Winglet

To enhance thrust performance, a winglet was integrated at the blade tip, which was extended to 92% of the blade radius. The winglet was then inclined at various angles—specifically 10°, 20°, 30°, 40°, 50°, and 80°. Both the tilt angle and the orientation of the winglet play a critical role in aerodynamic behaviour and thrust generation. To identify the optimal winglet configuration for maximum thrust output, nine distinct design cases were evaluated. The geometric configurations of these cases are illustrated in Figure (3), while Table (1) presents the classification of each winglet design along with the corresponding results obtained from (CFD) simulations.

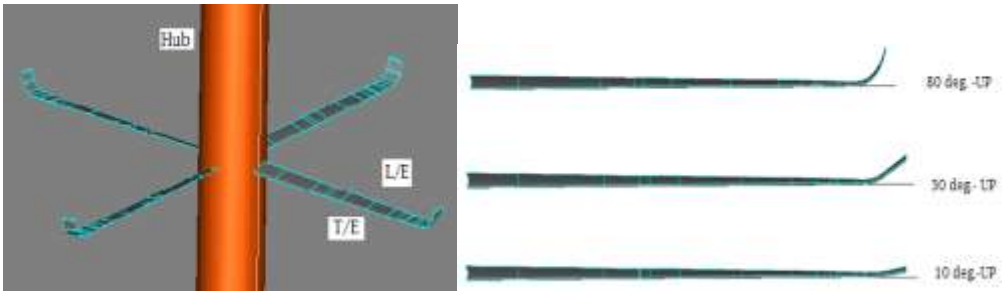

Figure3 : Different winglet configurations and Winglet at 80 degrees of UH-60A.

2.3. Mesh Generation and CFD Simulations

A three-dimensional (3D) structured mesh was developed using the NUMECA (AutoGrid) mesh generation tool. To simulate the aerodynamic interaction within a multi-blade environment, the mesh for a single blade was constructed under periodic

boundary conditions, effectively replicating the influence of adjacent blades. The final computational domain comprises approximately 9 million cells, as detailed in Table(1).

The thickness from the first grid point to the wall was estimated when V_{ref} = 213 (m/s), L_{ref} = 0.0924 (m) and ν =1.7e-5 (m^2/s). Assuming that if we wish to get y^+ around 1 at the wall, it turns out that Y = 2 x 10^{-6} (m). The range y^+ is appropriate for the tested turbulence models.

Table 1: Mesh quality of UH-60 Blade

Entire Mesh	8,893,898
Around the blade	5,750,243
Far Field	3,225,655

At mid-span, the 2D mesh of the blade has been illustrated in Figure (4), which has 16 blocks, and all of them stand together for the blade and the external field mesh. It habeen illustrated in Figure (4).

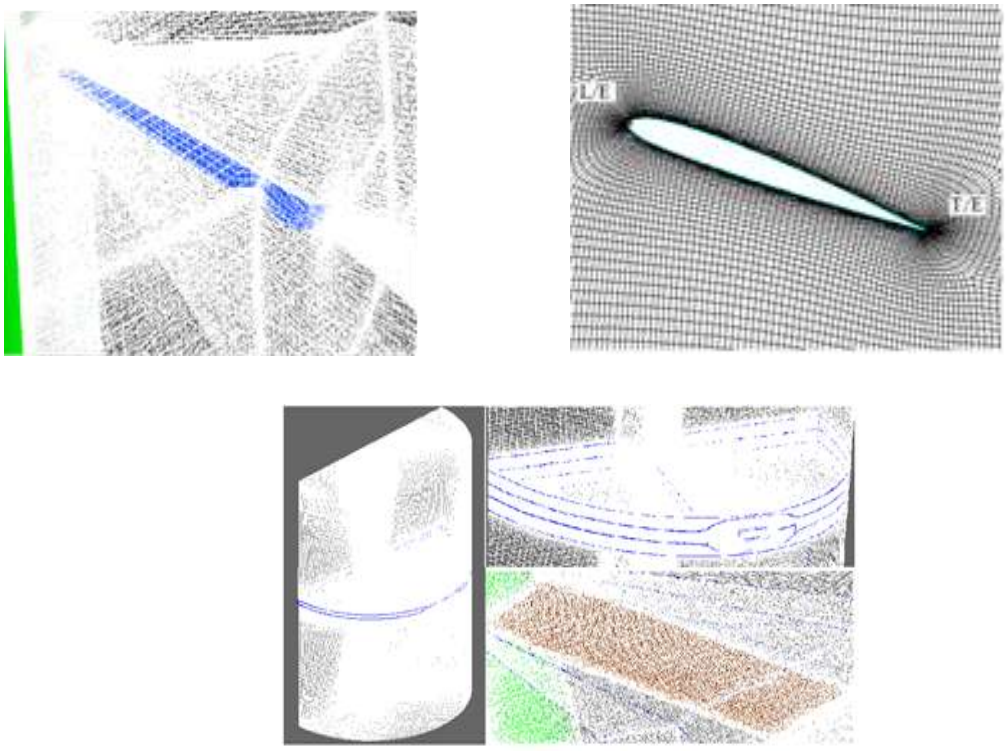

Figure 4:The 2D and 3D mesh at blade mid-span of UH-60 helicopter rotor blade.

The CFD results are validated against the experimental data in terms of the pressure coefficient distribution at different sections along the blade in Figure (5)[12]. There is a good match in general between the CFD results and the experimental data with small discrepancy at the outboard spanwise sections.

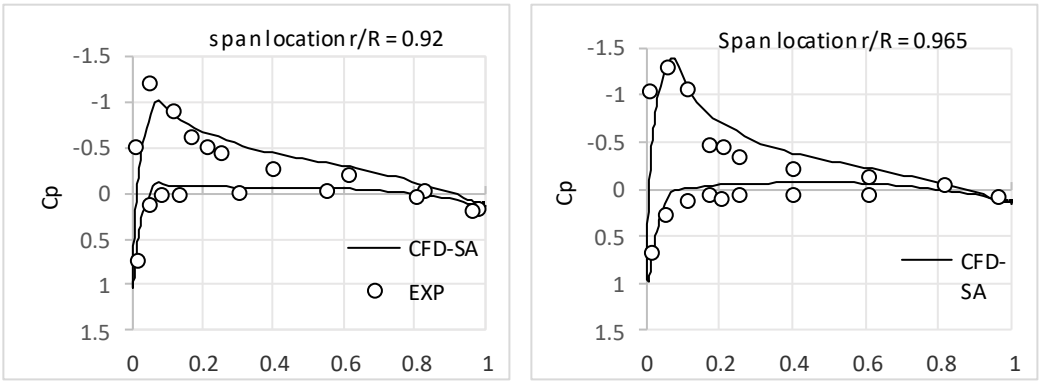

Figure 5. Comparison of Pressure coefficient for UH-60A.

2.4. Winglet Study and Result

The Reynolds-Averaged Navier–Stokes (RANS) equations were solved to evaluate the aerodynamic performance, employing the Spalart–Allmaras turbulence model for flow prediction. The simulation was conducted at a rotor rotational speed of 1425 RPM, with a collective pitch angle $\theta_{0.75} = 10.47°$ measured at 75% of the blade span, and a coning angle $\beta = -2.31°$.

Calculating the percentage of increase in thrust and the percentage of decrease in torque and also the figure of merit (FM) for winglet angle configurations is significant in determining the rotor performance. The figure of merit is defined in Equation 5.

$$FM = \frac{C_T^{3/2}}{\sqrt{2}C_Q} \tag{5}$$

where C_T and C_Q are the thrust and torque coefficients respectively.

Higher thrust generation is better for the hovering condition. However, more torque generation means that more power is needed to attain that thrust, which makes the helicopter less efficient.

Calculating figure of merit increase is important because that happens because of varying winglet configurations, and it also helps calculating the thrust increase/increment percentage as well as torque reduction percentage for comparing results with the original blade geometry. Every considered configuration has been listed in Table (2).

Table (2) shows the winglet classifications and the CFD results of the different cases. It is clear from the results that the addition of the proposed winglet has usually negative effect on the rotor performance. Only when using a winglet of 20-deg tilted towards the upper surface, the thrust has increased by around 2%. However, at the same time, the torque has increased by 2.3%.

Table 2**.** The winglet results.

Winglet angle (deg.)	Winglet direction	FM (%)	Thrust (%)	Torque (%)
10	up	0.95	1.911	-1.906
20	down	-1.77	0.000	-1.763
20	up	0.68	2.051	-2.338
30	down	-5.71	-1.538	-3.633
30	up	-1.90	1.678	-4.424
40	up	-2.04	1.399	-4.137
50	up	-4.08	1.305	-6.259
80	down	-20	-5.734	-14.424
80	up	-11.7	0.886	-14.676

3. CONCLUSION

In this study, the effect winglet angle and winglet direction for UH60A blade rotor has been analysed in terms of thrust force, Torque and figure of merit. Analyses have been performed for the same rotational speed value. Various cases are generated by allowing the change winglet angle and direction to tip rotor. The results of the addition of different winglet configurations to the have demonstrated little effects. The thrust force was improved by around 2%. However, the torque was noticed to increase in all the studies winglet cases.

REFERENCES

[1] Whitcomb R.T. July 1976 “A Design Approach and Selected Wind-Tunnel Results at High Subsonic Speeds for Wing- Tip Mounted Winglets”, NASA TN D-8260.

[2] Whitcomb R. T., 16 September 1981, “Methods for Reducing Aerodynamic Drag,” NASA Conference Publication 2211, Proceedings of Dryden Symposium, Edwards, California.

[3] J. E.Yates, and C. Donaldson, 1986 ,“Fundamental Study of Drag and an Assessment of Conventional Drag-Due-To-Lift Reduction Devices,” NASA Contract Rep 4004.

[4] Maughmer, M.D., June 2001, “The Design of Winglets for High-Performance Sailplanes,” AIAA Paper 2001-2406.

[5] Monier Ali ElFarra, January 2011 “Horizontal Axis Wind Turbine Rotor Blade Winglet And Twist Aerodynamic Design And Optimization Using CFD”, Ph.D., Aerospace Engineering Department.

[6] Thomas, F., 1999 ,“Fundamentals of Sailplane Design”, Translated by Judah Milgram, College Park Press, MD.

[7] Falk, T.J. and Matteson, F. H., 1971, “Sailplane Aerodynamics”, American Soaring Handbook, Soaring Society of America,.

[8] V.Madhanraj), Kaka Ganesh Chandra, Desineni Swprazeeth, Battina Dhanush Gopa, (2021), 1-9 ,” Design and Computational Analysis of Winglets”, Turkish Journal of Computer and Mathematics Education, Vol.12 No.7.

[9] M. Dinar, A. Leminos and M. Shephard. 1997, "Adaptive Solution Procedures for Rotorcraft Aero-dynamics." Rensselaer Polytechnic Institute, Rotorcraft Technology Center, Troy, NY, USA,.

[10] M. Potsdam, H. Yeo and W. Johnson,2006." Rotor Airloads Prediction Using Loose Aerodynami- cal/Structural Coupling." Journal of Aircraft 3(43):732 - 742,.

[11] W. G. Bousman. 2003 ,"Aerodynamic Characteristics of SC1095 and SC1094 R8 Airfoils." NASA TP-2003-212265, Aeroflightdynamics Directorate U.S. Army Research, Development, and Engineering Command Ames Research Center Moffett Field, CA, USA.

[12] Hweda Sharif, Ali Belhaj, Khaled.A.Aljaly, 2022 April.," The Effects of Sweep Angles and Sweep Angle Locations on twisted blade of Helicopter", Al academia journal for Basic and Applied Sciences (AJBAS) volume 4.